remote sensing

MDPI

Article

Satellite-Based Sea Ice Navigation for Prydz Bay, East Antarctica

Fengming Hui [1,2], Tiancheng Zhao [1], Xinqing Li [1], Mohammed Shokr [3], Petra Heil [4], Jiechen Zhao [5], Lin Zhang [5] and Xiao Cheng [1,2,*]

1 State Key Laboratory of Remote Sensing Science, College of Global Change and Earth System Science, Beijing Normal University, Beijing 100875, China; huifm@bnu.edu.cn (F.H.); zhaotc100@126.com (T.Z.); lixinqing0710@163.com (X.L.)
2 Joint Center for Global Change Studies, Beijing 100875, China
3 Science and Technology Branch, Environment Canada, Toronto, ON M3H5T4, Canada; mo.shokr.ms@gmail.com
4 Australian Antarctic Division and Antarctic Climate and Ecosystems Cooperative Research Centre, University of Tasmania, Hobart, TAS 7001, Australia; Petra.Heil@utas.edu.au
5 Key Laboratory of Research on Marine Hazards Forecasting (SOA), National Marine Environmental Forecasting Center, Beijing 100081, China; zhaojcsd@hotmail.com (J.Z.); linzh-60@nmefc.gov.cn (L.Z.)
* Correspondence: xcheng@bnu.edu.cn

Academic Editors: Weimin Huang and Prasad S. Thenkabail
Received: 14 March 2017; Accepted: 17 May 2017; Published: 24 May 2017

Abstract: Sea ice adversely impacts nautical, logistical and scientific missions in polar regions. Ship navigation benefits from up-to-date sea ice analyses at both regional and local scales. This study presents a satellite-based sea ice navigation system (SatSINS) that integrates observations and scientific output from remote sensing and meteorological data to develop optimum marine navigational routes in sea ice-covered waters, especially in areas where operational ice information is usually scarce. The system and its applications are presented in the context of a decision-making process to optimize the routing of the RV *Xuelong* during her passage through Prydz Bay, East Antarctica during three trips in the austral spring of 2011–2013. The study assesses scientifically-generated remote sensing ice parameters for their operational use in marine navigation. Evaluation criteria involve identification of priority parameters, their spatio-temporal requirements in relation to navigational needs, and their level of accuracy in conjunction with the severity of ice conditions. Coarse-resolution ice concentration maps are sufficient to delineate ice edge and develop a safe route when ice concentration is less than 70%, provided that ice dynamics, estimated from examining the cyclonic pattern, is not severe. Otherwise, fine-resolution radar data should be used to identify and avoid deformed ice. Satellite data lagging one day behind the actual location of the ship was sufficient in most cases although the proposed route may have to be adjusted. To evaluate the utility of SatSINS, deviation of the actual route from the proposed route was calculated and found to range between 165 m to about 16.0 km with standard deviations of 2.8–6.1 km. Growth of land-fast ice has proven to be an essential component of the system as it was estimated using a thermodynamic model with input from a meteorological station.

Keywords: sea ice; remote sensing; marine navigation; Antarctica

1. Introduction

Accurate knowledge of the sea ice distribution is crucial for ship navigation in polar-regions. Marine vehicles should follow safe and fast tracks in ice-rich waters. Severe ice conditions can significantly reduce the progress or even beset a vessel. The variability of sea ice conditions, especially

near the Antarctica coast, is often complex and transient as it is driven by synoptic atmospheric forcing or changing ocean currents, then modified by ice compression, divergence, shear or a mixture of all forms of deformation [1,2]. In recent years, several vessels have been delayed or entrapped in the Antarctic sea ice. These vessels were often surrounded by highly concentrated pack ice under compression accompanied with bad weather and snowstorms (e.g., the RV *L'Astrolabe* (France) in November 2009, RV *Xuelong* (China) in January 2010 and December 2013, and RV *Aurora Australis* (Australia) in November 2012).

In order to plan for a smooth and fast navigation in ice-covered waters, information about sea ice concentration (SIC), sea ice extent (SIE), sea ice thickness (SIT) and deformation such as ridges is needed. The SIC and SIT may be combined with the vessel's ice-strengthened class to develop a regulatory standard in ice-cover water, which is the essence of the Arctic Ice Regime Shipping System to provide mariners with information to navigate vessels safely through the sea ice [3]. However, no similar system exists for marine navigation in the Antarctic sea ice. Therefore, it has become essential to develop a system to support a safe nautical route for marine vehicles travelling in the Antarctic.

SIT can be estimated from microwave remote sensing but the estimation is limited to an upper limit of 16–50 cm pending on the frequency band [4]. Sea ice type identified in radar remote sensing images using surface features can be used as a proxy indicator of thickness of thicker ice. The spatio-temporal distribution of SIT in the Antarctic region was estimated using laser altimetry data from NASA's (National Aeronautics and Space Administration) Ice, Cloud, and land Elevation Satellite (ICESat) combined with passive microwave measurements during 2003–2008 [5]. Furthermore, a dataset of ice thickness for six regions around the Antarctic was developed by comprising 23,373 ship-based observations obtained over more than two decades [6]. None of these datasets, however, is suitable for marine operational use. For one thing, long-term average data do not represent the current ice thickness at locations that ship navigators require. Moreover, the problem with the satelite altimeter (radar or laser) is the narrow swath combined with a long repeat cycles (hundreds of days), which require numerous orbits to compile the thickness over a given area.

For seasonal ice, high values of SIE and extensive SIC may cause slowing down of a marine vehicle but are not likely to impede its motion unless the ice becomes highly deformed. Charts of SIC are generated daily at a few centers, based passive microwave observations and only occasionally based on synthetic aperture radar (SAR) data. The spatial resolution of the charts varies from a few kilometers to a few tens of kilometers. This may not be appropriate for navigation in highly variable regions such as eastern rim of Prydz Bay. As for the SIE, recent studies [7,8] have shown that since 1978, SIE around the Antarctic continent has demonstrated an increasing trend of $1.5 \pm 0.4\%$ per decade. The increase affects the breadth of the marginal ice zone around the Antarctica, a region of interest to ice navigation. Unlike the Arctic region, only a few routine sea ice analyses are available for the Antarctic regions [9,10]. This is partly due to the limited marine traffic in this region.

The Chinese National Antarctic Research Expedition (CHINARE) Program has been operating since 1984. Now there are four Chinese stations in Antarctica including Great Wall Station (built in February 1985), Zhongshan Station (built in February 1989), Kunlun Station (built in January 2009), and Taishan Station (built in February 2013) (Figure 1). The first two stations operate all year, and the latter two stations currently only operate in austral summer because of severe weather conditions. RV Xuelong has carried out the logistic support and personnel exchange annually for the four stations since 1994. En route in Prydz Bay, the vessel mostly encounters first-year sea ice (FYI) with typical thickness of 0.5–1.0 m [11,12]. Closer to the coast, namely within the last 30 km of the journey the vessel enters a land-fast ice regime. Most of this ice is thermodynamically-grown FYI with thickness between 1.5 m and 2.0 m [13,14]. Many icebergs calving from nearby ice shelfs can be grounded in the Bay, locally modifying the sea ice conditions. This complex setting provides challenges to ice navigation.

In this study we developed a satellite-based sea ice navigation system (SatSINS) for RV *Xuelong* navigation in the Prydz Bay. The system utilizes ice information obtained from visual analysis of space-borne remote sensing data, satellite-driven SIC charts, estimated SIT from a thermodynamic

model, and relevant meteorological data. This combination reveals key information about ice conditions and subsequently assists in developing a route for the ship. The later task implies a hypothesis that the availability of the aforementioned scientific products should facilitate the planning of the route. This hypothesis has been tested during three voyages of RV *Xuelong* to Zhongshan Station in the spring (November) of 2011–2013. The test involves calculation of the deviation of the planned route (output from SatSINS) from the actual route (adjusted by the ship masters), which was based on immediate observations of the ice field in the vicinity of the ship. SatSINS would be an additional asset to prepare for the growing forecast of human activities and their impacts on the Antarctic region, which are primarily motivated by the Antarctic explorations by nations and commercial tourism.

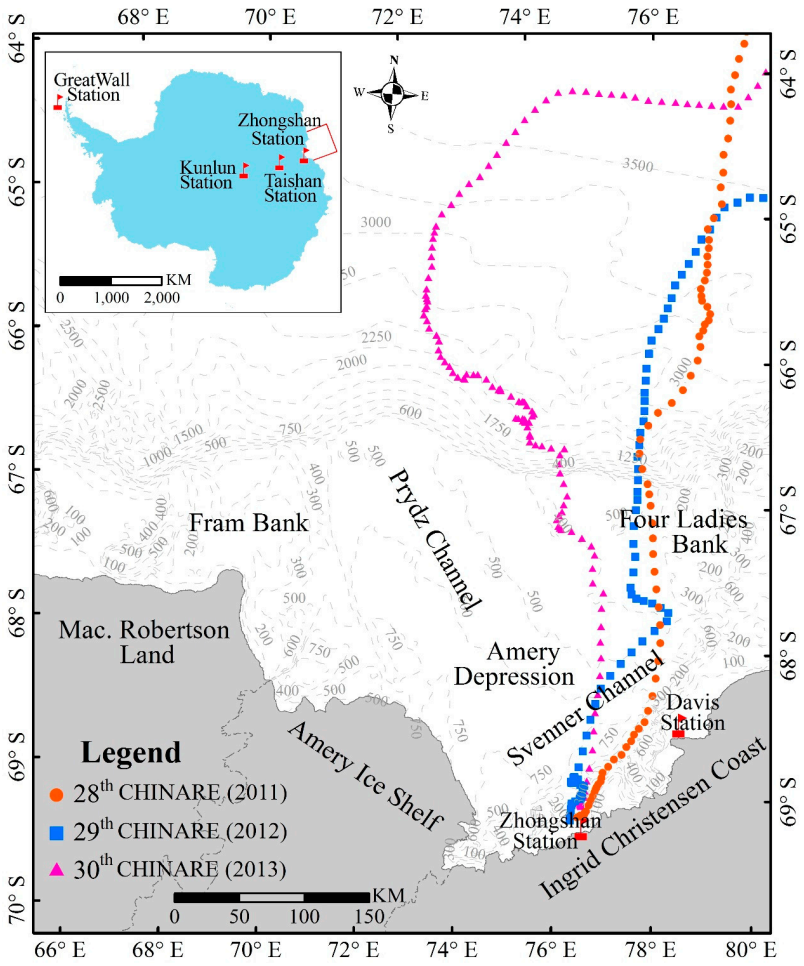

Figure 1. RV *Xuelong* navigation region in Prydz Bay outside Zhongshan Station. Cruise tracks for the 28th (2011, red), 29th (2012, blue), and 30th (2013, magenta) CHINARE are shown. The inset shows the locations of all four Chinese Antarctic research stations. CHINARE: Chinese National Antarctic Research Expedition.

2. Materials

2.1. Study Area

Prydz Bay is located in the Indian Ocean sector of the Southern Ocean between 66°E and 79°E (Figure 1). In late November, the outer edge of pack ice can reach approximately 63–64°S, some 600 km transit distance to Zhongshan Station. Large inter-annual variability of the sea ice conditions exists in the region due to complex bathymetry and water-mass distribution as well as the ocean–sea ice interaction [15]. The average thickness of drift ice and land-fast sea ice are typically 0.7 m and 1.4 m,

respectively. On average, transecting in the drift ice zone takes 2–4 days, followed by 1–3 days of breaking through the land-fast ice to the anchorage location off Zhongshan Station.

2.2. RV Xuelong Ice Navigation and Position Data

RV *Xuelong* is a polar ice-strengthened research vessel (Class B1) serving the four CHINARE research stations in the Antarctic. Every year, the ship arrives at the outer ice edge off Zhongshan Station, Prydz Bay, in late November or early December for the annual resupply. Its speed through the sea ice strongly depends on the SIC (Figure 2). In the open ocean its cruise speed may be up to 18 knots, but once in ice-covered seas, her progress slows down gradually with increasing ice cover. The navigation speed reduces significantly once SIC exceeds 70%. Maintaining a speed of 1.5 knots the RV *Xuelong* can break through 0.9-m-thick level ice with a 0.2-m snow load. Ice conditions with SIC > 95% and SIT > 1.0 m will typically block the ship's travel (Quan Shen, Captain of RV *Xuelong*, personal communication). Hence, optimal navigational routing is critical to minimize delays due to environmental conditions.

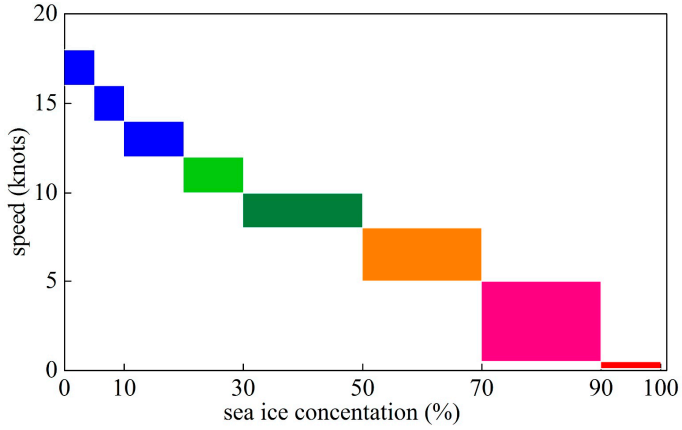

Figure 2. RV *Xuelong* navigation speed (knots) versus sea ice concentration in the Prydz Bay. Data are based on previous RV *Xuelong* sailing in the region.

The half-hourly samples of latitude, longitude, speed, and heading of RV *Xuelong* were utilized to assess the impact of sea ice conditions during the travel. The different routes across the Prydz Bay during the 28th, 29th and 30th CHINARE voyages are indicative of the large inter-annual variability encountered during the Novembers from 2011 to 2013 (Figure 1).

2.3. Remotely Sensed Data

The remotely sensed data include two sets of original imagery data and one set of the retrieved ice concentration from the brightness temperature data. The first set is true-color images from the moderate-resolution imaging spectroradiometer (MODIS) comprising three bands: 1, 4 and 3 with wavelength 645 nm, 555 nm, and 469 nm, respectively. Image sharpening using Band 1 is applied to Bands 4 and 3 to obtain composite color images at 250 m resolution [16].

The second set is high-resolution C-Band SAR data. We accessed both ASAR (Advanced Synthetic Aperture Radar) data from the European Envisat (available prior to its decommissioning in April 2012) and SAR data from the Canadian Radarsat-2. In general, SAR data has a limited coverage (100–500 km swath width), which reduces their availability at specific times and locations. For this study of ice navigation in Prydz Bay four ASAR and two Radarsat-2 SAR images were acquired (Table 1). SAR images were obtained at level 1B, which were then georeferenced, calibrated and speckle filtered. Image processing was implemented using ESA's (European Space Agency) NEST (the Next ESA SAR Toolbox) software at Beijing Normal University (BNU). The map projection was UTM (Universal Transverse Mercator) Zone 43S with WGS84 Datum. The calibrated images (radar backscatter (σ°) in

decibels; dB) were sent to ice pilots on board RV *Xuelong*. All remote sensing data were transformed into layers and analyzed in ArcGIS 10.0 software. It is noted that when near-coincident SAR data were not available, MODIS imagery was used instead.

Table 1. Synthetic aperture radar (SAR) imagery used for ice navigation in Prydz Bay (2011–2013) *.

CHINARE	Sensor	Pixel Spacing (m × m)	Acquisition Time (Coordinated Universal Time, UTC)	Polarization Mode	Beam Mode	Swath Width (km × km)
28th (2011)	Envisat ASAR	75 × 75	19:25 22 November 2011 19:16 25 November 2011 18:39 26 November 2011 19:42 27 November 2011	HH	Wide Swath	400 × 400
30th (2013)	Radarsat-2 SAR	50 × 50	22:45 27 November 2013 15:14 29 November 2013	HH + HV	ScanSAR Wide	500 × 500

* SAR imagery was not ordered in 2012 because sea ice concentration (SIC) was less than 70%.

The third set is made up of daily SIC maps, generated using the Arctic Radiation and Turbulence Interaction Study (ARTIST) Sea Ice (ASI) algorithm [17]. Data from the 91 GHz channel of the Special Sensor Microwave Imager/Sounder (SSMIS) were used for the maps of the 28th CHINARE (in 2011) and data from the 89 GHz channel of the Advanced Microwave Scanning Radiometer 2 (AMSR-2) were used for the maps of the 29th and 30th CHINARE (in 2012 and 2013). Grid spacing of 6.25 km is maintained for both cases.

2.4. Meteorological Data

Meteorological data used in this study included 3-hourly atmospheric forecasts of mean sea level pressure (MSLP), near-surface winds from the Antarctic Mesoscale Prediction System (AMPS), and daily air temperature from an automatic weather station (AWS) in Zhongshan Station. AMPS data are available at a grid size of 15 km with high quality [18] and were validated for the Antarctic [19]. This dataset has been used to support wind forecasting and air operations, both inter- and intracontinental, especially in rescues and emergency situations as well as scientific field campaigns and activities. The MSLP and surface wind data reveal information about the expected weather system that will prevail over the ice regime at the time when the vessel enters it. The decision to acquire fine-resolution SAR data for ice navigation is based on this forecast. Daily air temperature is used to estimate the growing thickness of land-fast using a simple thermodynamic model.

3. SatSINS

The SatSINS is composed of three modules: "Prior to reaching ice edge", "Approaching ice edge"; and "In ice" (Figure 3). Each module is bounded with time, ice condition and ship location.

The addressed ice conditions include SIE (to determine when the vessel will enter the ice-covered water), SIC, ice types, approximate SIT in the bay (to determine the arrival time to the final destination) and the local-scale sea ice variability near the coast (to ensure smooth arrival to the destination). Ice extent, concentration and variability are mainly remote sensing issues, while ice thickness is mostly a thermodynamics issue that can better be estimated using a thermodynamic model (unless thickness develops as a result of ice crushing and piling in highly dynamic regimes). Stefan's Law of ice growth [20] was used in this study to estimate the land-fast ice thickness.

The analysis of sea ice conditions took place at three phase that signifies different scales of information in relation to the location of the vessel relative to the ice cover. The first is when the vessel is 2–3 weeks away from the ice, the second is when the vessel is approaching the ice edge (about one

week from reaching the final destination) and the third is when the vessel navigates through the pack ice. The analysis procedures are summarized in the flow chart (Figure 3). Each module represents one analysis phase. Data downloading and analysis were performed by the team members residing at BNU as land coordinators.

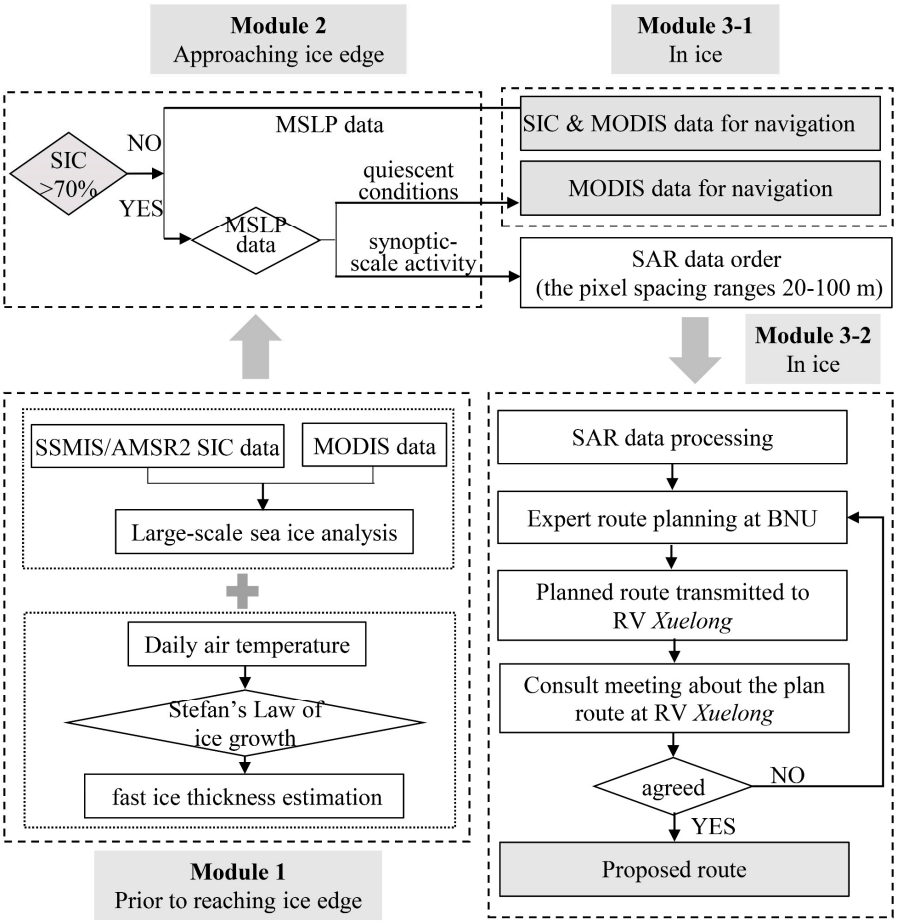

Figure 3. Flow chart of the SatSINS system with its three modules. SatSINS: satellite-based sea ice navigation system; MODIS: moderate-resolution imaging spectroradiometer; BNU: Beijing Normal University; MSLP: mean sea level pressure; SSMIS: Special Sensor Microwave Imager/Sounder.

3.1. Module 1: Landfast Ice Thickness Estimation and Large-Scale Sea Ice Analysis

3.1.1. Analytical Ice Model for Fast Ice Thickness

The land-fast ice thickness was calculated prior to ice navigation. This was usually finished before November 20 when RV *Xuelong* departed from Australia after resupply. Since land-fast ice growth is a predominantly thermodynamic process, its thickness can be estimated using the continuity of heat flux from the underlying water to the atmosphere through the ice and snow layers. Assuming linear temperature profiles through the ice thickness and snow-free ice surface, the ice growth rate for a given thickness H is given by Stefan's law [20]. In this study, a modified version considering ice–atmosphere coupling [21] was used. The density of sea ice, the latent heat of freezing of sea ice, the thermal conductivity of sea ice, and the heat exchange coefficient were set to 910 Kg/m^3, 333.4 KJ/Kg, 2.2 W/(m°C), and 0.73 W/(m°C); respectively. The daily air temperature was obtained from AWS at Zhongshan Station. In agreement with observations of the freeze-up near Zhongshan Station [14], the calculation is initiated on 1 March with zero thickness. It should be noted that the above-mentioned model is based on the assumption of snow-free surface and zero ocean heat flux. Both assumptions

lead to conservative estimates of ice thickness (i.e., over prediction), which is favorable for the current application. Snow cover insulates the ice surface and thereby results in slower ice growth rate and overestimation of the thickness.

3.1.2. Large-Scale Sea Ice Analysis

This analysis was conducted during the first two weeks of the voyage. The data in Module 1 (Figure 3) includes georeferenced SIC maps from SSMIS/AMSR-2 data and MODIS true-color images. The large-scale sea ice characteristics are tracked to delineate the ice edge and broadly identify distinct ice features of the pack ice in the Prydz Bay, with a view to detecting possible navigation paths with benign ice conditions. It facilitates a later decision on whether finer resolution satellite data will be needed and may therefore be ordered. The analysis involved examination of daily SIC maps to identify any large-scale ice features. This was communicated daily to the vessel by the team at BNU. Cloud-free MODIS data were also used to verify the SIC derived from the passive microwave data. The ice-edge demarcation and the overall ice characteristics in the marginal ice zone and the pack ice in the Prydz Bay had to be verified. This process usually takes an hour after downloading the data.

3.2. Module 2: Analysis of Medium-Scale Sea Ice Characteristic

This analysis was conducted when RV *Xuelong* was approaching the ice edge. The data sources and the logical decisions are included in Figure 3. The 6-h MSLP data was integrated with the data from MODIS and the SIC maps to assess the severity of the ice conditions and the need for more details of ice conditions from SAR images to support navigational analysis of ice conditions in Prydz Bay.

According to RV *Xuelong* navigation information (Section 2.2), the vessel can travel quickly and safely in sea ice with SIC < 70% and she will travel slowly and even be trapped in SIC > 70% when the SIT exceeds 1.0 m. So if the regional SIC distribution in Prydz Bay is below 70%, there would be no need for further detailed information on the ice or the atmospheric conditions. In this case, SIC maps from SSMIS/AMSR-2 along with available MODIS images would be sufficient for the route planning. Note that sea ice modelling results and observation data indicate that the SIT does not exceed 1.5 m in the Bay, though it can be deformed and broken pieces accumulate to bring the thickness up to 3.0 m, as observed in the West Ice Shelf [11,12]. Ice thickness up to 1.5 m does not constitute an obstacle for RV *Xuelong* to travel and reach Zhongshan Station, though it would certainly slow her travel. However, if the SIC in Prydz Bay is over 70%, the need for high-resolution imagery is identified pending further information from the MSLP data. The information will identify a possible presence of cyclones or anti-cyclones over the region. If anti-cyclones are proven to exist, the atmospheric conditions in the bay will be largely quiescent and cloud-free. In this case, MODIS data will be sufficient (as a fine-enough resolution data source) to provide the ice information for the vessel's route planning. Alternatively, if the MSLP data reveal several consecutive cyclones passing by the bay, it means that clouds prevail and the turbulent atmospheric conditions will cause higher mobility of sea ice and therefore more surface deformation. This condition, combined with an estimate of SIC > 70%, triggers the need for the higher resolution SAR images. Consequently, in our examples, either Envisat or Radarsat-2 images were acquired in Wide-Swath or ScanSAR modes (Table 1). The imagery would be available within 2 h of the satellite overpass.

3.3. Module 3: Analysis of Fine-Scale SAR Data and the Final Ship-Route Planning

Subjective interpretation of SAR images was performed to identify sea ice types (with a proxy evaluation of ice thickness), concentration and surface deformation. Meteorological data were used in support of the visual images analysis. The images were then annotated with GPS (Global Positioning System) points of a proposed route and typically sent as 4-Mbyte data bundles to RV *Xuelong*. The suggested route was reviewed by the CHINARE team, taking into consideration the local conditions of the nearby sea ice as observed from the vessel. If the proposed sea ice route was deemed to be suitable after the review, RV *Xuelong* would proceed along the proposed waypoints. Otherwise an improved

route plan was requested by the ship-board party. Access to near-real-time remote sensing data (6–8 h as required by the operational ice-monitoring centers) was not a strict requirement for developing the proposed route as discussed in the next two sections.

The processing chain to derive a full iteration of route planning and assessment takes about 2–3 h. Incorporation of SAR data is the slowest element in the process. It takes about half hour to download a single image, one to one and half hour to process the data and identify key ice conditions, and another half hour to transfer the proposed routes to RV *Xuelong*. This time lag needs be taken into account when developing the proposed route, especially if the MSLP and wind data confirm the possibility of rapid changes of sea ice conditions.

4. Results

SatSINS was used for ice navigation in November 2011–2013 in support of the RV *Xuelong* as she approached the ice edge by the second half of November during each year (Figure 4). Over 2014–2016, on the other hand, SIC in the region were low, and the SatSINS procedures were similar to those taken in 2012. The SIC showed inter-annual variability which can be reflected very well by RV *Xuelong* ice navigation speed (Figure 4). Large scale MSLP and 10-m wind field on selected days during CHINARE ice navigation periods are presented in Figure 5. The large-scale atmosphere circulation features are useful since they will impact the ice drift pattern and eventually affect preorder of SAR data in the SatSINS.

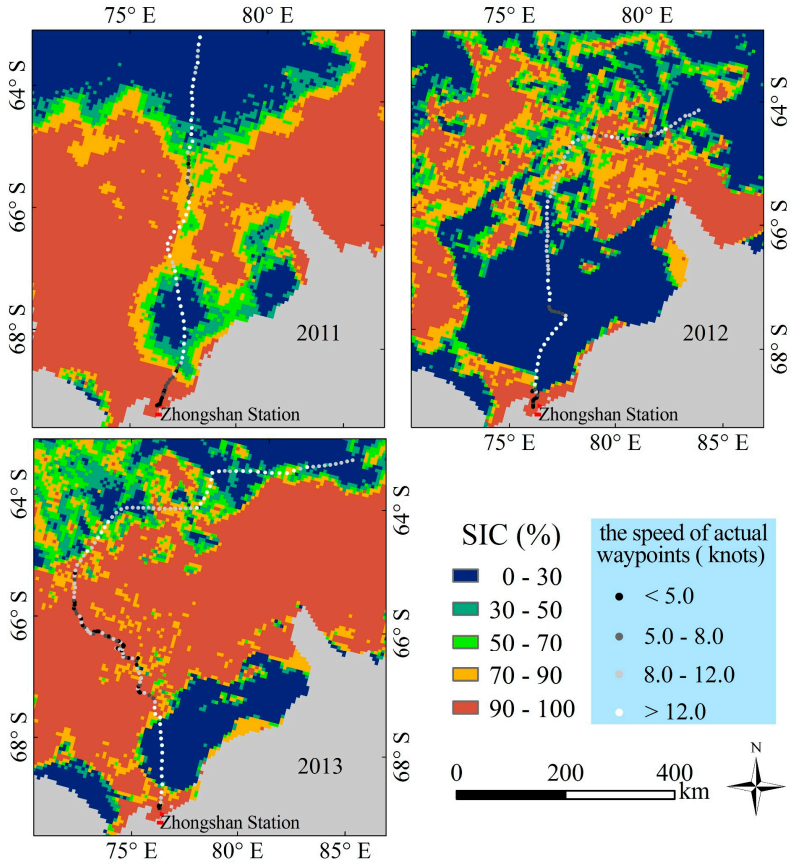

Figure 4. Sea ice concentration from the Special Sensor Microwave Imager/Sounder (SSMIS)/Advanced Microwave Scanning Radiometer 2 (AMSR2) for Prydz Bay on 23 November for each expedition: 2011, 2012 and 2013. The vessel track is overlaid as sequence of points coded with colors to indicate the speed.

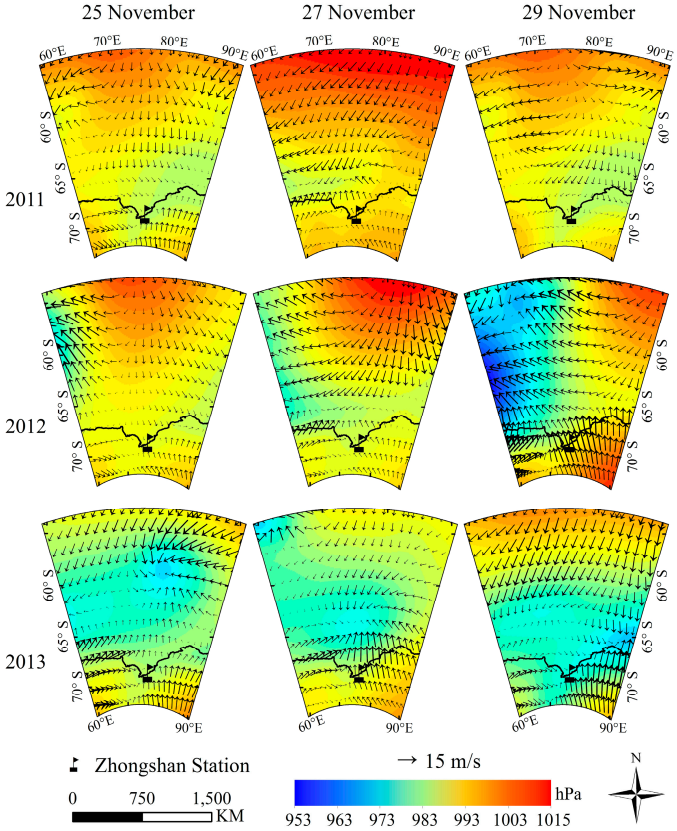

Figure 5. Six-hour MSLP fields (color) with 10-m wind vectors, at 00:00 UTC on 25, 27 and 29 November in 2011–2013.

4.1. Navigation through Landfast Ice

Typically, the extent and average thickness of the land-fast ice off Zhongshan Station are approximately 30 km and 1.5 m in early December. Under these conditions RV *Xuelong* was in full ice breaking operation in a land-fast ice zone. The highest risk was the grounded ice ridges and icebergs, which can often be detected by the ice crew onboard. The seasonal variation of land-fast ice thickness between March and November during the 2011–2013 was estimated using a modified version of Stefan's law (as mentioned before). Results are presented in Figure 6. The average air temperature between March and November during the 2011–2013 seasons are −11.6 °C, −11.9 °C, and −12.4 °C, respectively. The maximum land-fast ice thickness in the three years remained around 1.6 m. The maximum ice thickness in November is a proxy to be taken into account on whether a higher class ice breaker would be needed to assist RV *Xuelong*.

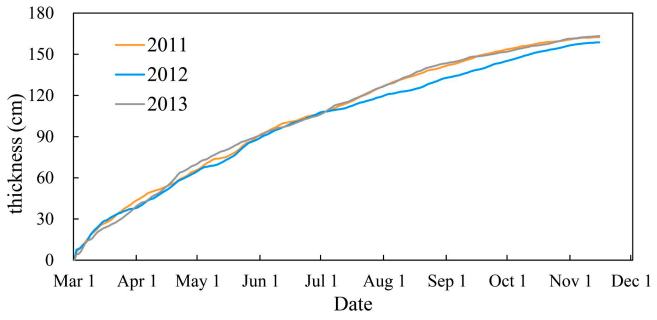

Figure 6. Land-fast ice thickness based on modified version of Stefan's law from 1 March to 15 November 2011–2013.

4.2. CHINARE2011 Ice Navigation

Ice concentration in Prydz Bay was generally above 90%, while there was a region between 77°E and 78°E with SIC as low as 70% at some latitudes in November 2011 (Figure 4). A small open-water area existed between these two longitudes around 68°S. A ridge of high atmospheric surface pressure moved north of Prydz Bay from 25 to 29 November, imposing some minor modifications to the regional MSLP distribution (Figure 5, top). Quiescent conditions (25 November) changed to moderate (wind speed less than 10 ms^{-1}) on 27 November and 29 November with similar benign weather forecast for the following days. The ice conditions and the associated weather patterns triggered a request for SAR.

On 27 November a proposed route with 20 waypoints was sent to RV *Xuelong* based on the sea ice analysis of ASAR-WSM (Wide Swath Mode) images acquired on 25 and 26 November when RV *Xuelong* entered into the sea ice region at approximately 63.5°S, 77.5°E (Figure 7). She was advised to enter the sea ice zone east of 76°E. Consequently, with slight adjustments to the proposed route, she progressed smoothly at a speed of 3.4 to 14.8 knots through the pack ice zone.

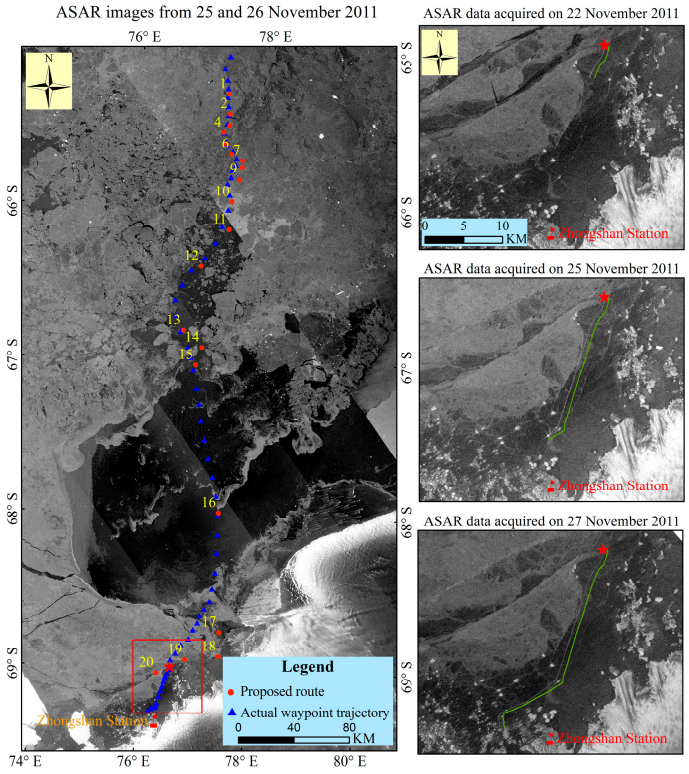

Figure 7. ASAR images acquired on 25 and 26 November 2011 (left), with the navigation points of RV *Xuelong* (blue) from 27 November to 29 November 2011 and the 20 planned waypoints (red). The waypoints were based on analysis of the ASAR images. Images at the right are enlargement of the area marked by the red box in the left panel on different days, showing the progress of the wake of the Russian icebreaker through the land-fast ice off the Zhongshan Station.

A narrow bright straight line was barely visible in the ASAR images of 22, 25 and 27 November (Figure 7), contrasting the darker signature of the surrounding smooth land-fast ice. It started as a 7-km short line on 22 November and extended further south within the land-fast ice to just north of Zhongshan Station by 25 November before turning to the Indian Bharati Station (76.19°E, 69.40°S) on 27 November. This was interpreted as a narrow refrozen lead or a rough ice track of a vessel. As RV *Xuelong* approached this feature, communication with staff at Bharati Station confirmed that the Russian icebreaker *Vladimir Ignatyuk* had provided icebreaking support for MV (Motor Vessel) *Ivan Papanin*, resupplying the station. It was then confirmed that the bright line represented an opening

with water and broken ice in the wake of the Russian ice breaker. Consequently, after leaving the 16th waypoint, RV *Xuelong* changed course to follow that opening. This led to abandonment of the proposed waypoints 17 and 18. Entering the lead through the fast ice on 29 November, she moved at an average speed of 3.5 knots (with a maximum speed of 7.7 knots), following the lead towards the Zhongshan Station to all but the last 10 km of land-fast ice.

To assess the performance of the sea ice routing, we calculated the deviation of the actual trajectory of the vessel from the proposed route. This ranged from 165 m to 25.3 km with a standard deviation of 6.1 km. However, with the exclusion of the waypoints 17 and 18 as described before, the range reduced to a maximum of 6.9 km and the standard deviation to 2.8 km.

4.3. CHINARE2012 Ice Navigation

Ice concentration was low in the bay during the austral summer of 2012. RV *Xuelong* took 3 days (28–30 November) to navigate from the ice edge to her anchorage point 25 km north of Zhongshan Station. The SIC was less than 70% in most parts of Prydz Bay (Figure 4), with lower concentration (less than 50%) in the area between 76° and 78°E, and between 64° and 66°S. This area featured the merge of two polynyas; Barrier Bay and Prydz Bay as confirmed in a coincident MODIS image (Figure 8). The low SIC favors utilization of MODIS images without further consideration of the expensive SAR images. The low SIC, however, may subject to rapid retreat of sea ice distribution in response to the weather conditions.

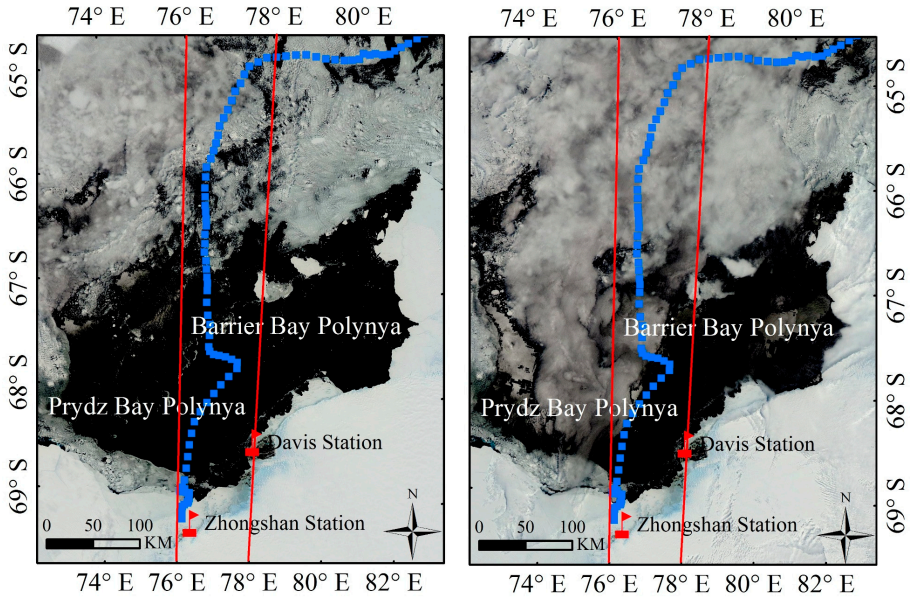

Figure 8. Sea ice in the region of interest as seen in composite Terra and Aqua MODIS imagery acquired on 23 November (**left**) and 25 November (**right**), 2012. The blue squares are the navigation GPS points of RV *Xuelong* from 28 November to 3 December 2012. The zone delineated by the two red lines presents the boundaries of the recommended sector for the route (no waypoints were proposed).

On 25 November the outer boundary of an anticyclone with a wind speed of less than 5 ms^{-1} was situated over the Prydz Bay, and a low pressure trough had moved over the bay by 27 November (Figure 5). On 29 November a cyclone with its center near 60°S, 60°E moved east. With expected increase of wind speed during the cyclone overpass, the SIC was expected to further decrease though the ice surface deformation would intensify. The latter factor was not crucial to incorporate in the route planning as the ice cover appeared to be relatively thin. Operation of SatSINS advised RV *Xuelong* to travel in the region between 76°E and 78°E, heading south of 66.5°S to reach the Prydz Bay Polynya by 28 November. This route ensured avoidance of unfavorable changes in the sea ice cover due to the

approach of the low-pressure system (Figure 8). RV *Xuelong* took about 23 h at an average speed of 10.2 knots to pass through sea ice to the polynya. On the afternoon of 29 November she experienced blizzard conditions, with wind speed peaking at 27 ms^{-1}. On 30 November the vessel had to wait to be escorted by the Russian ice breaker through the 25 km of the land-fast ice to the final destination.

It is worth reiterating that only the MSLP reanalysis and surface wind forecasts are needed to develop a route when the ice types and concentration do not seem to be hazardous (<70%). That is to ensure that the strong wind, associated with a possible cyclonic pattern, will not disturb the ice cover which has been estimated from maps generated a few days ago. This approach was not used in the case of the CHINARE2011 because ice concentrations of less than 70% were encountered. The ice conditions in November 2012 demonstrated that daily MODIS imagery can be used together with passive microwave.

4.4. CHINARE2013 Ice Navigation

Ice concentrations in the Bay exceeded 90% in November 2013, which is considerably higher than the previous years, with barely any leads visible (Figure 4). MODIS imagery acquired on 20–29 November confirmed this distribution. Therefore, the SatSINS process recommended that SAR data had to be ordered to guide the nautical sea ice analysis. On 25 November, a cyclone centered at approximately 78.5°E, 59.5°S (Figure 5) moving southeast from the northern Prydz Bay was soon followed by second cyclone moving eastward from the western Prydz Bay (53.8°E, 63.2°S). A third, albeit weaker, cyclone was located over the bay on 27 November moving to the east, and two other cyclones covered Prydz Bay on 29 November. Winds at RV *Xuelong* location were quiescent (less than 5–6 ms^{-1}) and clouds prevailed from 27 to 30 November. This suggested that sea ice conditions were unlikely to have changed greatly by that time.

The two Radarsat-2 images acquired on 27 and 29 November (Figure 9) showed very large ice floes across almost the entire ice pack with a number of very small leads once south of 65°S (hundreds of meters to a few kilometers in length). It appeared impossible for RV *Xuelong* to navigate through the compact pack ice region without detailed ice distribution and a proposed route based on remote sensing data. Though part of the Prydz Bay was cloud-covered on 29 November, a MODIS image was sufficiently clear over the region of interest to identify ice floe boundaries and a few leads. Consequently, a route with 12 waypoints was first proposed based on information from the MODIS data, recommending RV *Xuelong* sail towards 65°S, 73°E and from there travel along the defined zone in a southeasterly direction towards Zhongshan Station (Figure 9). The waypoint information was sent to the vessel on 29 November. At 20:00 (UTC) of the same day a refined route with 13 waypoints was derived according to sea ice conditions obtained from Radarsat-2 SAR image acquired at 15:14 (UTC) (less than 5 h from vessel entry into the ice in Prydz Bay) (Figure 9). The differences between the waypoints of the first and second proposed routes were minor. The SAR image was acquired one day before the start of the vessel's path shown in Figure 9. Therefore, it is possible that the vessel encountered ice distribution slightly different from the one based on MODIS data only. For most of the route, the vessel speed was between 8 and 12 knots. Figure 9 includes a line separating an areas of ice cover with leads (concentration < 90%) and an area of fully consolidated ice (100%). Locations of a few selected points on that line were included in the proposed route with an advice for the vessel not to cross over it into the fully consolidated pack. The SAR-based route follows locations of apparent leads or thin ice. The deviation of the actual route from the first route ranged between 1.5 km and 15.7 km, with a standard deviation of 4.2 km. For the second route, the deviation ranged between 245 m to 11.0 km with a standard deviation of 3.0 km.

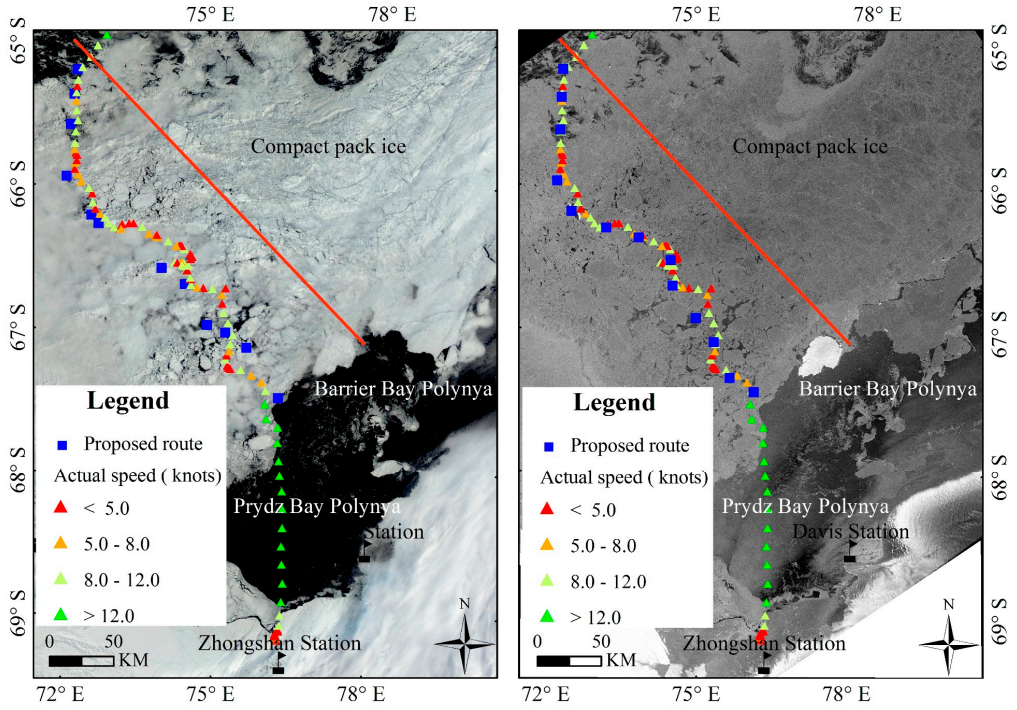

Figure 9. The ice-covered Prydz Bay from MODIS (**left**) and Radarsat-2 SAR HH polarization imagery (**right**), both acquired on 29 November 2013. The waypoints of the proposed routes are shown by the blue squares, and the navigation GPS (Global Positioning System) points of RV *Xuelong* from 30 November to 2 December 2013 are overlaid by the colored triangles, where colors are indicators of the vessel speed as displayed in the legend. The red line separates an area of 100% ice concentration (fully consolidated ice) to the north-east and another area of less than 100% with apparent leads.

Because the region east of 75°E was almost 100% ice concentration, navigation of RV *Xuelong* was considered risky without any satellite-assisted sea ice analysis. The vessel succeeded in passing through the pack ice at an average speed of 5.7 knots over 2 days along the proposed route, arriving at the fast-ice edge within 22 km of Zhongshan Station at 19:30 (UTC) on 2 December 2013.

5. Discussion

The success of the proposed nautical route is assessed based on the travel time of the vessel to reach its destination. A journey is hampered when the vessel's speed is less than 1 knot. The use of remote-sensing-driven ice parameters and the meteorological data in SatSINS proved to be successful in avoiding this situation. Ice conditions, navigation parameters and deviation of the actual ship route from the planned route for the three expedition are summarized in Table 2. In all cases, the vessel travelled at an average speed of 5.7 knots or higher in pack ice. However, the SatSINS-proposed routes needed adjustments based on local observations from the ship, especially when severe atmospheric/oceanic conditions triggered variations in the ice cover at a short time scale (i.e., within a few hours). This adjustment, along with the average speed of the ship during her navigation through the ice cover, are used to assess the utility of remote sensing and meteorological information for planning an efficient route. Here we discuss a few ice parameters/processes that impede the ship navigation (represented in terms of key navigation parameters) and the degree of success of SatSINS in offering solutions. A few recommendations for generating more and better operational-oriented scientific products are also presented.

Table 2. Summary of ice navigation for CHINARE2011, CHINARE2012 and CHINARE2013.

Expedition	Mobile Ice Synoptic	Fast Ice [#]		Speed in Pack Ice (Knots)		Speed in Fast Ice (Knots)		Navigation Duration (Hours)			Deviation from Planned Route [&]	
		Thickness (m)	Extent (km)	Average	Standard Deviation (Stdev.)	Average	Stdev.	Pack Ice	Fast Ice	Total *	Range	Stdev. (km)
2011	Concentration > 90% in most areas, with region of 70% and a limited open water area	1.2–1.61	28	9.9	3.3	3.5	1.7	15	43	69	165 m–25.3 km	6.1
											165 m–6.9 km	2.8
2012	Concentration < 70% in most parts, lower concentration in area of merged polynyas	1.23–1.55	20	10.2	1.9	3.7	1.7	23	33	125	-	-
2013	Concentration > 90%, barely any lead visible. Quiescent wind conditions, no significant change in ice conditions	1.22–1.58	21	5.7	3.6	2.6	1.6	48	69	130	245 m–11.0 km	3
											1.5–15.7 km	4.2

[#] The land-fast ice information was measured by scientists in Zhongshan Station prior to the CHINARE expedition in late October and early November. * The total navigation duration included the navigation time in Prydz Bay Polynya. [&] In 2011, the first group data is calculated by 20 waypoints, and the second group data is from 18 waypoints (exclusion of the waypoints 17 and 18). In 2013, the first group data is calculated from 13 waypoints in SAR data, and the second group data is from 12 waypoints in MODIS data.

As explained before, analysis in SatSINS starts with examination of coarse-resolution SIC daily maps. This is performed in conjunction with the analysis of a medium-resolution imagery data (MODIS data) to develop a synoptic description of the ice conditions (concentration, types, floe size, etc.) particularly in areas of high ice concentrations. This first-cut information is used to: (1) provide the expected location of the ice edge; (2) identify the synoptic ice conditions that will be encountered; (3) support a decision on whether there is a need for better timely and finer-resolution SAR images to develop a route through hazardous ice cover. The system continues with examining meteorological data to estimate possible deformation of the ice cover, and fine-resolution remote sensing data to assess the deformation and the ice types in ice-risk areas. Five scientific questions related to geophysical forces that impede navigation, along with their relevant navigation variables, are addressed in the rest of this section.

Question 1: What are the priority ice parameters that should be evaluated to the benefit of the ship navigation in ice-covered water?

As presented in Section 1, the four parameters needed to plan for a safe nautical route are (in a descending order of priority): SIT, SIC, SIE and ice surface deformation (which may be manifested as a local increase in ice thickness). SIC is useful in providing a synoptic-scale description of the ice regime. Ice thickness is calculated occasionally from thermal infrared or passive microwave sensors yet with an upper limit of 0.2 m except when using for the L-band microwave which retrieves a thickness up to 0.5 m. Absence of ice thickness data represents a challenge in developing a nautical route. An example is demonstrated in CHINARE2012 when the vessel had to navigate through 25 km of land-fast ice to reach its final destination. A most practical method for an approximate estimate of ice thickness is by identifying ice-types in remote sensing images and use it as a proxy indicator of the thickness. However, this does not apply to the land-fast ice because unlike other ice-types this is not a thickness-based category; i.e., it exists with a wide range of thickness and age. It can only be estimated approximately using a thermodynamic model.

Lack of accurate ice-thickness estimation may render the ice-concentration information of limited value. The case of CHINARE2013 illustrates this point when information about 100% ice concentration is provided, yet without ice thickness information, which is more critical for developing the nautical route. In this case, the decision on the way points of the route was guided by the locations of the apparent clusters of leads and openings in the close pack ice (the dark spots in the SAR image in Figure 9). The advantage of using SAR in identifying the iceberg in this particular case should also be noted.

Empirically speaking, the relative risk posed by different ice conditions to the structure of a ship is mainly determined by combining SIT and SIC. The combination may be represented in the form of an "ice numeral", which is the sum of the product of ice concentration of each type (mostly thickness-based) and an ice multiplier (a value that combines the ice types and the category of the vessel) [3]. Scientifically speaking, ice mechanical properties such as tensile, flexural, shear and compressive strength are prime parameters that impact the vessel's speed in relation to its power [22]. So far it is not possible to use the physical properties of sea ice (e.g., brine pocket spacing, brine volume and crystallographic information) to estimate these loads. Instead, empirical equations have been developed to estimate flexural and tensile strength in terms of porosity and brine volume, respectively [23]. Another set of equations that describes the loads exerted by creep failure against a structure was developed [24]. All of these equations are developed for the Arctic region with no parallel equations for the Antarctic ice. Moreover, most of these equations deal with thermodynamically-grown ice only without considering ice thickening due to mechanical deformation. The limit of their applicability is ice of up to 2 m [24]. Lack of ice mechanical properties in the Antarctic region has been a motivation for development of the SatSINS.

The system takes into consideration two particular ice features. The first, which generally applies to Antarctic sea ice, is the absence of perennial ice. This type is far more hazardous than seasonal

ice. The second is that ice mechanical strength of seasonal ice (that dominates around the Antarctica) decreases by about 50% of its value in the spring compared to mid-winter values (as measured in the Canadian Arctic). In comparison, the strength of perennial ice decreases by only 10–20% of its mid-winter value [23]. SatSINS was developed for marine navigation in seasonal ice during the spring season, where ice strength is not at its peak. This also relaxes the requirements of ice information from remote sensing.

Ice deformation, in terms of ridging that represents hazard for some ships or openings that represent safe navigational routes, is a key parameter in the planning of the nautical route. Ridging not only increases the ice thickness but also the loading on the ship structure. Radar remote sensing, with its fine resolution (e.g., the spatial resolution ranges from 20 to 100 m) and sensitivity to surface roughness and structure, provides the required information though only qualitatively. This is part of the procedures in the SatSINS. It enables a flexible framework to assist in decision-making for the route planning yet the best information is still generated by ship masters based on local ice observations. For a given ice concentration, the weight of its impact on the ship structure is doubled if the ice is deformed by ridges, rubble or hummocking. On the other hand, it may be reduced by half for decayed ice [3].

It should be noted that ice parameters critically needed for ice navigation can be highly variable (spatial- and temporal-wise), depending upon the climatological and local environmental history in the region (mainly wind and temperature). That was the motivation behind the inclusion of meteorological data in the system. Moreover, most of the readily available parameters for polar marine navigation are based on observations from the Arctic region. Ice climatology in the Antarctic is different in many ways; namely the type of pack ice, fast ice, perennial ice, polynyas, and the amount of highly deformed ice. Additionally, different site-dependent environmental conditions that dominate during initial ice growth such as air temperature, wind and oceanic conditions strongly affect key parameters that contribute to ice mechanical properties. Examples include ice crystalline structure (e.g., frazil or columnar), porosity, and bulk salinity. Obviously, many of these macroscopic parameters are too difficult to measure or retrieve to provide useful operational information. Therefore, only higher-level ice information is used in SatSINS.

Question 2: What are the spatio-temporal requirements from remote sensing data and the maximum allowable time gap between data acquisition and the actual operation?

Spatial resolution of remote sensing data is needed at two scales to reveal gross and detailed conditions of the ice cover. Coarse resolution images and daily SIC maps (a few kilometers in resolution) available 3–7 days before the vessel encounters the ice can be used to delineate ice edge and confirm whether SIC will exceed the threshold of 70% or not. Below this threshold, only medium-resolution imagery data from an optical sensor (250–500 m resolution) are likely to be sufficient to develop waypoints for a proposed vessel route. MODIS data were used in the case study of CHINARE2012 when most of the Prydz Bay was covered by thin ice within a large polynya. The only limitation here would be the availability of cloud-free images. Coarse resolution data are also needed to reveal the synoptic-scale ice picture. The Southern Ocean circumpolar currents causes the ice cover to spread freely off shore, covering a wide area.

Fine resolution data, on the other hand, are needed for a few purposes. The first is to estimate the average size of the ice floes. The probability of collisions of ice floes increases at higher ice concentration of smaller floes. This reduces the overall speed of the ice pack but exerts extra ice loads on the ship (assuming same ice type and thickness are encountered) due to repeated collisions with the smaller floes. The second is to obtain ice information in small water areas (e.g., polynyas and fjords). This was particularly important for the last phase of the RV *Xuelong* as it approached its destination. The data are also needed in regimes of highly-mixed ice types. Case studies of CHINARE2011 and CHINARE2013 demonstrate this situation. The spatial resolution of 75 m from ASAR and 50 m from

Radarsat-2 was sufficient to extract the required information, which is mainly about ice type, ridged zones (unfavorable features) and opening in the cover (favorable features).

Ice motion is the factor that dictates the requirement for the temporal resolution of ice information in regimes of high SIC. In open drift (SIC between 0.4 and 0.6), ice will move at a speed approximately three times higher than the motion of close pack ice (SIC between 0.9 and 1.0), yet it is not hazard for ship navigation. When pack ice moves freely in response to the wind, its speed approaches nearly two percent of the wind speed [25]. Faster motion is expected when the ice surface becomes rough. The steep topography and the presence of glaciers in the Antarctica's coastal areas create katabatic winds that intensify sea ice motion. The effect of the wind extends to within 40 km off shore. A data set of satellite tracked sea ice motion in the Antarctic for the period 1992–2010 is presented [26]. It links the statistically significant trends in Antarctic ice drifts (in most sectors) to local winds. Maps of sea ice motion with 48-h span and 62.5-km resolution are generated by the Ocean and Sea Ice program of the Satellite Application Facilities (OIS-SAF) of EUMETSAT (The European Organisation for the Exploitation of Meteorological Satellites) for limited areas in the west Antarctica winter. The 25-km EASE-Grid (the Equal-Area Scalable Earth Grid (EASE-Grid)) weekly sea ice motion around the Antarctica, available from the National Snow and Ice Data Centre (NSDIC), shows limited ice motion in the study area; typically around 3 km/day with anomalies that can reach 12 km/day [27]. Such large-scale gridded data are not useful for tactical ship navigation planning. Ice motion products from SAR data, with remarkable precision compared to products from passive microwave or scatterometers, are not useful also because of their poor temporal revisit coverage. In all cases, ice motion tracking cannot be estimated accurately during the ice melt season or at locations where variable atmospheric conditions cause decorrelation of the radiometric signature from one day to the next. The above discussions deliver a rationale for using the MSLP and near-surface wind data to reveal information about the severity of local ice motion and hence justify a decision to order fine-resolution SAR data.

The requirement for timely remote sensing data depends on the ice conditions revealed initially by the coarse resolution data. This issue can be illustrated using the key dates for each expedition (Table 3), which include arrival of the vessel to the ice-covered area, arrival to final destination and the acquisition time of the satellite images/products. It should be noted that in CHINARE2012 the journey ended on 3 December (arrival to the Zhongshan Station) after almost 6 days from entering the pack ice in Prydz Bay. However, RV *Xuelong* took only 2 days to cross the pack ice and the polynya (Figure 8) and nearly 4 days to cross land-fast ice ahead as mentioned before. The table also shows that the most up-to-date satellite data (which were used to develop /or adjust the proposed route) were acquired on the same day (in 2011 and 2013) or 3 days before the actual time of the vessel arrival in the imaged scene (in 2012). The decision was mainly based on the severity of ice dynamics (change within a few hours or a few days). In the case of CHINARE2012, when a large polynya covered most of the Prydz Bay, MODIS data acquired 3 days before the vessel entry to the bay was sufficient for the route planning. On the other hand, when the bay was covered by nearly 100% ice concentration in 2013, Radarsat-2 SAR image had to be ordered so that the acquisition date coincided with the time of the vessel's arrival at the sea ice edge. The route plan for the CHINARE2011 mission was based on Envisat images acquired 4 then 3 days before the vessel encountered the ice then adjusted based on a newly acquired image (2 days before the vessel encountered the ice).

The frequent changes in ice concentration, motion and re-distribution caused by the high wind speed in the Antarctic region warrants a need for higher temporal resolution of SAR imagery when planning for vessel routes. The case of CHINARE2011 illustrates the importance of availability of SAR data on daily basis even if the ice cover does not appear to change much. The ice scene in the three Envisat images acquired on 22, 25 and 27 November 2011 (the three images at the right side in Figure 7) does not change but the appearance and propagation of the thin bright line in the three images proved to be of particular importance as described before. In general, one SAR image per day would be sufficient. This revisit frequency has been available with the launch of Sentinel-1A in April 2014 and Sentinel-1B in in April 2016, comprising a constellation of the two satellites. The two-satellite

constellation could offer a 6-day exact repeat cycle. The SAR revisit frequency will be further enhanced with the launch of Radarsat Constellation Mission (RCM) scheduled in 2018 [28]. The increased revisit frequency will be a useful and welcomed improvement for route planning.

Table 3. Key dates of RV *Xuelong* navigation in the ice covered water in Prydz Bay and acquisition dates of the satellite and SIC map data

Year	November							December				
	22	**23**	**24**	**25**	**26**	**27**	**28**	**29**	**30**	**1**	**2**	**3**
2011	EN	SIC		EN	EN	***S*** EN		***E***				
2012		SIC MOD		MOD			***S***					***E***
2013	MOD	SIC MOD	MOD	MOD	MOD	RS MOD	MOD	***S*** RS MOD				***E***

S: start journey in ice cover; ***E***: end journey; SIC: sea ice concentration maps; EN: Envisat ASAR images; MOD: MODIS images; RS: Radarsat-2 images.

Question 3: What is the required level of accuracy of ice information?

Accuracy of existing SIC maps ranges from 5 to 20%, depending on the concentration-based categories of the ice cover, i.e., open drift, closed pack/drift, compact and consolidated, etc. [29]. The accuracy increases as ice age or thickness increases. This level becomes acceptable as long as the ice field is not subjected to severe changes at short time scale. Less accuracy is usually attached to scenes of dominant thin ice-types such as open and closed pack drift; usually encountered in polynyas and marginal ice zones. Nevertheless, the accuracy is not a crucial issue in this case since navigation through thin ice is not a challenge for ice breakers. As for the ice type information obtained through subjective analysis of remote sensing data (SAR or optical sensors), the accuracy cannot be established. The navigational route plan can then rely on such unverified analysis, supported by SIC maps and ship observations. When changes in the ice cover take place at a fast rate under severe weather conditions the question of the accuracy becomes irrelevant and any planned route will be subject to adjustments; which can sometimes be substantial.

Question 4: Is there a need for data integration from different sensors?

A single-channel SAR may not be very useful in discriminating between open water and thin ice cover as in the case of polynya (Figure 9). The radar backscatter from thin ice and open water overlap heavily because each surface has a wide range of backscatter signature. Signature of thin ice is affected by: (1) surface salinity, which varies significantly with thickness during the early ice growth stage, as well as the presence of frost flowers; and (2) surface roughness, which is manifested in a few forms such as rafting. On the other hand, open water exhibits a range of backscatter signature starting from very low values when the water surface is calm to high values when the surface becomes turbulent in response to wind action. This ambiguity does not exist in optical remote sensing data (e.g., in MODIS images) since the surface roughness does not affect the radiance from sea water. Integration of optical and radar imagery is important in this case. Another supporting observation is the identification of the iceberg in the SAR image (Figure 9 near the middle of the image) compared to its vague appearance in the MODIS image. Large grain size of the iceberg's snow cover trigger high backscatter in SAR data [30]. Acquisition of multi-polarization SAR data is recommended to solve the ambiguity of SAR signature of open water. Recent studies concluded that backscatter in cross-polarization SAR is always low regardless of the wind-driven surface roughness [31]. These data will be more available for commercial use in the future.

Question 5: How can a remote-sensing-driven route be evaluated against possible adjustments based on ship observations of the surrounding ice?

According to ship-based observations of surrounding ice, the planned route may have to be adjusted while moving through sea ice as in the cases of CHINARE2011 and CHINARE2013 expeditions (Figures 7 and 9, respectively). The maximum deviation of the actual route from the planned waypoints was nearly 7 km and 3.5 km with standard deviation of 2.8 km and 3.0 km in 2011 and 2013, respectively. These numbers are justified based on typical values of ice motion (2–6 km per day), when the observations used to develop the proposed nautical route is one or days lagging behind the actual operation time. Higher deviation from the planned route is expected when the vessel encounters a highly dynamic ice regime with intensive spatio-temporal variation of ice cover.

6. Conclusions and Recommendations

This study presents a system, called SatSINS, for using a suite of remote sensing data to devise a proposed nautical route for vessel navigation through sea ice cover in the Southern Ocean. This task was undertaken because of the lack of a regulatory ship navigation system in the Antarctic waters (unlike Arctic waters) and the limited availability of ice information there. The system is presented in the context of a decision-making process to support the routing of the Chinese RV *Xuelong* during her passage through Prydz Bay. We demonstrated that different remote sensing and meteorological data sources and products play diverse roles in providing sea ice information at different spatial and temporal scales. A few factors that contribute to the gap between demand and supply data for nautical ice navigation are discussed. Our study has presented how such gap can be narrowed, underlining the importance of case studies to provide guidance on how to best chain a suite of satellite data for the use of nautical ice navigation. Discussions of navigation parameters that meet conditions of geophysical processes that impede ship navigation are presented.

Coarse-resolution data including SIC maps and medium resolution optical imagery provide synoptic scale ice information. This information is used to delineate the ice edge and synoptic features of the ice field. If large-scale ice concentration is less than 70% then only SIC and optical data (e.g., from MODIS) are sufficient to develop a proposed nautical route. Otherwise, fine-resolution SAR data should be analyzed to identify ice features that should be avoided (e.g., thick and ridged ice zones) and features that should be included in the proposed route (e.g., leads and thin ice). Atmospheric forecast data of MSLP and near surface wind should be examined in both cases to assess the severity of ice conditions and therefore the need for inclusion of SAR data (only if SIC > 70%). The information on cyclone systems (initial location, development, and movement routes) was vital for RV *Xuelong*'s navigation.

In this study the closest available satellite data to the actual location of the vessel were lagging by one day. In most cases that was sufficient but the proposed route may have to be adjusted based on observations of the surrounding ice from the ship. To assess the performance of the proposed routing, we calculated the deviation of the actual trajectory of the vessel from the proposed route. For the 28th CHINARE2011, the maximum deviation was nearly 7 km and for the 30th CHINARE2013 the average deviation was 3.5 km. This is consistent with possible ice redistribution caused by its mobility. When the major part of the vessel's route was covered by thin ice in a polynya (29th CHINARE2012) the vessel was advised to travel within a proposed meridional band rather than along specific waypoints.

The parameters needed to develop the vessel route in ice-covered water include SIC, SIT, ice-type distribution, and ice deformation (triggered by ice motion). While ice concentration is readily available at a coarse resolution, ice type and surface deformation are usually retrieved subjectively through visual image analysis, particularly of SAR data. Ice thickness is the most difficult parameter to estimate, especially after the ice grows beyond a few weeks. This is particularly true in the case of land-fast ice because this ice has a wide range of thickness. The slowest speed experienced by RV *Xuelong*'s was during her navigation in the land-fast ice near Zhongshan Station. Thickness of this ice was calculated using a simple thermodynamic model and air temperature available from an existing meteorological

station. Accurate estimates of sea ice thickness on a short time scale from remote sensing to satisfy navigational requirements still need considerable improvement.

It is recommended to pursue research into mechanical properties of sea ice in the Antarctic and to develop a regulatory ship navigation system, similar to the Arctic Ice Regime Shipping System, by combining the vessel's ice-strengthened class with the ice thickness and concentration.

Acknowledgments: This work was supported by Chinese Arctic and Antarctic Administration, National Natural Science Foundation of China (41676176, 41676182 and 41428603), Chinese Polar Environment Comprehensive Investigation and Assessment Program. PH was supported by Australian Antarctic Science grants 4072 and 4301 as well as by the Antarctic Climate and Ecosystems CRC program. RV *Xuelong*'s nautical data were accessed via the "*XUELONG* Online" website (http://Xuelong.chinare.cn/Xuelong/). We are grateful to the European Space Agency for providing ASAR data, the Institute of Environmental Physics at University of Bremen of Germany for providing daily sea ice concentration data, NASA for providing daily MODIS mosaic imagery of Antarctica and the Polar Meteorology Group at Byrd Polar Research Center of The Ohio State University for providing AMPS forecast data. The 1:500,000 bathymetric data are courtesy of the Australian Antarctic Data Centre. Last but not least, the authors wish to thank the anonymous reviewers who did a thorough critical review of the manuscript and provided valuable suggestions to improve it.

Author Contributions: F.H. conceived and designed the experiments, and wrote the manuscript; T.Z. and X.L. processed and analyzed the data; J.Z. and L.Z. collected field data and discussed the results; M.S. and P.H. investigated the results and revised the manuscript; X.C. investigated the results, revised the manuscript and supervised this study.

Conflicts of Interest: The authors declare no conflict of interest.

References

1. Heil, P.; Hutchings, J.K.; Worby, A.P.; Johansson, M.; Launiainen, J.; Haas, C.; Hibler, W.D., III. Tidal forcing on sea-ice drift and deformation in the western weddell sea in early austral summer, 2004. *Deep Sea Res. Part II Top. Stud. Oceanogr.* **2008**, *55*, 943–962. [CrossRef]
2. Comiso, J.C. Variability and trends of the global sea ice cover. In *Sea Ice*, 2nd ed.; Thomas, D.N., Dieckmann, G.S., Eds.; Wiley-Blackwell: Hoboken, NJ, USA, 2010; pp. 205–246.
3. Transport Canada. *Arctic Ice Regime Shipping System (AIRSS) Standards*; Transport Canada: Ottawa, ON, Canada, 1998; Volume TP 12259E.
4. Shokr, M.; Sinha, N. *Sea Ice: Physics and Remote Sensing*; John Wiley & Sons, Inc.: Hoboken, NJ, USA, 2015; p. 623.
5. Kurtz, N.; Markus, T. Satellite observations of antarctic sea ice thickness and volume. *J. Geophys. Res* **2012**, *117*, C08025. [CrossRef]
6. Worby, A.P.; Geiger, C.A.; Paget, M.J.; Van Woert, M.L.; Ackley, S.F.; DeLiberty, T.L. Thickness distribution of antarctic sea ice. *J. Geophys. Res Oceans* **2008**, *113*, C05S92. [CrossRef]
7. Zwally, H.J.; Comiso, J.C.; Parkinson, C.L.; Cavalieri, D.J.; Gloersen, P. Variability of antarctic sea ice 1979–1998. *J. Geophys. Res Oceans* **2002**, *107*, 3041. [CrossRef]
8. Parkinson, C.L.; Cavalieri, D.J. Antarctic sea ice variability and trends, 1979–2010. *Cryosphere* **2012**, *6*, 871–880. [CrossRef]
9. Wang, X.; Cheng, X.; Hui, F.M.; Cheng, C.; Liu, Y.; Sum, H.K. Xuelong navigation in fast-ice near the zhongshan station, antarctica. *Mar. Technol. Soc. J.* **2014**, *48*, 84–91. [CrossRef]
10. Zhai, M.; Li, X.; Hui, F.; Cheng, X.; Heil, P.; Zhao, T.; Jiang, T.; Cheng, C.; Ci, T.; Liu, Y.; et al. Sea ice conditions in the adélie depression during besetment of the chinese icebreaker RV *Xuelong*. *Ann. Glaciol.* **2015**, *56*, 160–166. [CrossRef]
11. Guo, J.; Sun, B.; Tian, G.; Wang, B.; Zhang, X. Research on electromagnetic inductive measurement of sea-ice thickness in antarctic prydz bay. *Chin. J. Geophys.* **2008**, *51*, 596–602. [CrossRef]
12. Li, Q.; Wu, H.; Zhang, L. Fine-Scale Simulation of the Seasonal Variations of Sea Ice Cover in the Prydz Bay, Antarctic. *Acta Oceanol. Sin.* **2011**, *33*, 32–38. (In Chinese).
13. Heil, P.; Allison, I.; Lytle, V.I. Seasonal and interannual variations of the oceanic heat flux under a landfast antarctic sea ice cover. *J. Geophys. Res. Oceans* **1996**, *101*, 25741–25752. [CrossRef]
14. Lei, R.; Li, Z.; Cheng, B.; Zhang, Z.; Heil, P. Annual cycle of landfast sea ice in prydz bay, east antarctica. *J. Geophys. Res Oceans* **2010**, *115*, C02006. [CrossRef]

15. Gao, G.; Dong, Z.; Shi, M.; Liu, H. Advances of physical oceanographic study on prydz bay and adjacent region, antarctica. *J. Shanghai Ocean Univ.* **2013**, *22*, 313–320. (In Chinese).
16. Gumley, L.; Descloitres, J.; Schmaltz, J. Creating Reprojected True Color MODIS Images: A Tutorial. 2010. Available online: ftp://ftp.ssec.wisc.edu/pub/IMAPP/MODIS/TrueColor/ (accessed on 20 July 2016).
17. Spreen, G.; Kaleschke, L.; Heygster, G. Sea ice remote sensing using amsr-e 89 ghz channels. *J. Geophys. Res.* **2008**, *113*, C02S03. [CrossRef]
18. Powers, J.G.; Manning, K.W.; Bromwich, D.H.; Cassano, J.J.; Cayette, A.M. A decade of antarctic science support through amps. *Bull. Am. Meteorol. Soc.* **2012**, *93*, 1699–1712. [CrossRef]
19. Bromwich, D.H.; Otieno, F.O.; Hines, K.M.; Manning, K.W.; Shilo, E. Comprehensive evaluation of polar weather research and forecasting model performance in the antarctic. *J. Geophys. Res. Atmos.* **2013**, *118*, 274–292. [CrossRef]
20. Stefan, J. Über die theorie der eisbildung, insbesondere über die eisbildung im polarmeere. *Ann. Phys.* **1891**, *278*, 269–286. [CrossRef]
21. Leppäranta, M. A review of analytical models of sea-ice growth. *Atmos. Ocean* **1993**, *31*, 123–138. [CrossRef]
22. Weeks, W.F.; Assur, A. The mechanical properties of sea ice. In *USA Cold Regions Research and Engineering Laboratory, Monograph II-C3 1967*; Cold Regions Research & Engineering Laboratory: Hanover, NH, USA, 1967.
23. Timco, G.; Weeks, W. A review of the engineering properties of sea ice. *Cold Reg. Sci. Technol.* **2010**, *60*, 107–129. [CrossRef]
24. Timco, G.; Johnston, M. Ice loads on the caisson structures in the canadian beaufort sea. *Cold Reg. Sci. Technol.* **2004**, *38*, 185–209. [CrossRef]
25. Thorndike, A.; Colony, R. Sea ice motion in response to geostrophic winds. *J. Geophys. Res. Oceans* **1982**, *87*, 5845–5852. [CrossRef]
26. Holland, P.R.; Kwok, R. Wind-driven trends in antarctic sea-ice drift. *Nat. Geosci.* **2012**, *5*, 872–875. [CrossRef]
27. Tschudi, M.; Fowler, C.; Maslanik, J.; Stewart, J.S.; Meier, W. *Polar Pathfinder Daily 25 km Ease-Grid Sea Ice Motion Vectors, Version 3*; National Snow and Ice Data Center: Boulder, CO, USA, 2016.
28. Thompson, A.A. Overview of the radarsat constellation mission. *Can. J. Remote Sens.* **2015**, *41*, 401–407. [CrossRef]
29. Manual of Ice (MANICE). *Manual of Standard Procedures for Observing and Reporting Ice Conditions, Canadian Ice Service*; Environment Canada: Toronto, ON, Canada, 2005; ISBN 0-660-62858-9. Catalogue No. En56-175/2005.
30. Drinkwater, M.; Long, D.; Bingham, A. Greenland snow accumulation estimates from satellite radar scatterometer data. *J. Geophys. Res. Atmos.* **2001**, *106*, 33. [CrossRef]
31. Vachon, P.W.; Wolfe, J. C-band cross-polarization wind speed retrieval. *IEEE Geosci. Remote Sens. Lett.* **2011**, *8*, 456–459. [CrossRef]